Development of Test Facility and Optical Instrumentation for Turbulent Combustion Research

D.R. Ballal,* A.J. Lightman,† and P.P. Yaney‡
University of Dayton, Dayton, Ohio

Practical combustion systems as complex as a gas turbine combustor, a ramjet, or an afterburner pose many design and modeling difficulties. This has created an urgent need for well conceived turbulent combustion experiments to validate the models and to improve their potential design capabilities. With that broad goal in mind, the U.S. Air Force Wright Aeronautical Laboratories, Aero Propulsion Laboratory initiated a major program with the University of Dayton Research Institute to 1) develop a sophisticated combustion test facility, 2) develop state-of-the-art optical instrumentation capable of measurements in nonreactive and reactive turbulent flows, and 3) carry out well conceived turbulent combustion experiments. This paper describes the development of the combustion test facility and the optical instrumentation. A turbulent flame burner provides low exit turbulence (<0.25%), predictable velocity profile; and it is capable of producing a variety of flame configurations. A two-component LDA system, capable of measuring velocity fluctuations over three orders of magnitude, has been designed. A three-channel laser Raman/Rayleigh spectroscopy (LRS) system, which can simultaneously measure temperature, density, and species concentration, has been constructed. Integration of the LDA-LRS systems is carried out to measure complex correlations between velocity, temperature, concentration, and density in a turbulent flame. Design and development of auxiliary systems and equipment such as fuel and airflow networks, LDA seeders, and the flow visualization system are described in detail.

Nomenclature

b	= equivalent bar size ($\approx 0.95d$)
c	= concentration, area contraction ratio
d	= diameter of hole
g	= acceleration due to gravity
K	= constant
M	= mesh size
P	= pressure, probability density function (pdf)
$S_\alpha(\phi)$	= net mass formation rate through reaction of species α
T	= temperature
t	= time
u,v,w	= velocities in x, y, and z directions, respectively
x,y,z	= coordinate directions
ϕ_α	= mass fraction of species α
ρ	= density

Superscripts

$\tilde{(\ )}$	= density weighted (Favre) average
$\bar{(\ )}$	= conventional average
$(\ )''$	= fluctuation from Favre averaged value
$(\ )'$	= fluctuation from conventional averaged value

Subscripts

i,j	= tensor coordinates
α	= species

Background

CURRENT research in turbulent combustion has been motivated by a need for improved performance from compact combustors, their durability in an environment of high heat release rates, and reduced emissions of smoke and pollutants. Computer models to predict flowfield and combustion processes in a gas turbine combustor, a ramjet, or an afterburner are in an active stage of evaluation and development. Thus, in the future, the possibility exists that costly experimental combustor development programs can be shortened if not altogether eliminated.

The conservation equations of continuity, momentum, and a scalar (temperature or concentration) for a high-turbulence Reynolds number in a density weighted (Favre averaged) form are:

$$\frac{\partial \bar{\rho}}{\partial t} + \frac{\partial}{\partial x}(\bar{\rho}\tilde{u}_i) = 0 \tag{1}$$

$$\frac{\partial \bar{\rho}\tilde{u}_i}{\partial t} + \frac{\partial}{\partial x_j}(\bar{\rho}\tilde{u}_i\tilde{u}_j) = \bar{\rho}g - \frac{\partial \bar{P}}{\partial x_i} - \frac{\partial}{\partial x_j}(\widetilde{\bar{\rho}u_i''u_j''}) \tag{2}$$

$$\frac{\partial \bar{\rho}\tilde{\phi}_\alpha}{\partial t} + \frac{\partial}{\partial x_i}(\bar{\rho}\tilde{u}_i\tilde{\phi}_\alpha) = -\frac{\partial}{\partial x_i}(\widetilde{\bar{\rho}u_i''\phi''}) + \overline{\rho S_\alpha}(\phi) \tag{3}$$

To solve these and other relevant equations, modelers are often forced to make empirical, unjustifiable, or even erroneous assumptions. For example, the turbulence chemistry closure requires probability density function $P(\tilde{\phi},x)$ which is chosen somewhat arbitrarily; the turbulent transport process is often cast in the form of a turbulent eddy diffusivity, a concept increasingly under attack; and finally, the modeling of dissipation terms is empirical at best. Thus, both the utility and the applicability of models to the design of practical systems become limited.

The above discussion clearly suggests a need for well conceived experiments with controlled reproducible inlet boundary conditions to validate the models; see, for example, Roquemore.[1] The potential design capabilities of these sophisticated models can be fully realized only if the physics and the chemistry of "turbulent combustion" in both laboratory and practical combustor geometries are better understood. With that broad goal in mind, the Air Force Wright Aeronautical Laboratories, Aero Propulsion Laboratory (AFWAL/PO), Wright-Patterson Air Force Base,

Presented as Paper 86-0045 at the AIAA 24th Aerospace Sciences Meeting, Reno, NV, Jan. 6-9; received Jan. 30, 1986; revision received July 24, 1986.

*Senior Research Engineer, Research Institute. Associate Fellow AIAA.
†Research Physicist, Research Institute.
‡Professor of Physics and Electro-Optics. Member AIAA.

OH initiated a program, in 1983, with the University of Dayton Research Institute (UDRI). The following sections describe some aspects of this program.

Introduction

The program had the following main objectives: 1) develop a combustion test facility for relevant laboratory and practical combustion experiments; 2) develop state-of-the-art optical instrumentation capable of simultaneous, time resolved, point and multipoint measurements of velocity, density, temperature, and species concentration in nonreactive and combusting flows; and 3) carry out well conceived experiments to enhance the understanding of "turbulent combustion" and thus lead to advancements in the computer models and codes. The complexity of turbulent combustion dictated a multifaceted effort involving fluid mechanics, combustion, spectroscopy, optics, electronics, computer software, and interfacing, and demanded a strong interaction between theory and experiments.

Combustion Laboratory Facility

Figure 1 shows the layout of a combustion laboratory located in Building 490, Test Cell 153 of AFWAL. A distance of 4 ft separates the tables to provide a central access for the turbulent flame burner (TFB). The burner is mounted vertically on a three-axis traversing table as shown in the photograph of Fig. 2. It is capable of a vertical traverse of 2 ft and a traverse of 9 in. in each of the horizontal directions. A blower that delivers up to 2600 standard cubic feet per minute (scfm) (at 14 in. static pressure) supplies air to the burner. An exhaust hood connected to a 20-in.-diam pipe is located directly above the burner working section exit. The hood can be traversed manually between an 8–10 ft elevation as the burner moves. Its 2-ft-long skirt ensures a complete exhaust of burned products from the low-velocity combustion experiments.

Other features of the combustion laboratory are 1) safety provisions: Gas detectors are installed at strategic locations on the floor, in the ceiling, and on the side walls. All major electrical power circuits in the test cell are explosion proof. The laser power is interlocked with warning lights, and the gas detectors are interlocked with the audio warning, the ventilation system, and the fire alarm system; 2) climate control provision: High-quality optical components manufactured to close tolerances demand a temperature/humidity controlled environment. The combustion laboratory is equipped with air conditioning, humidity control, and steam-coil heater units so that a summer temperature of $75 \pm 5°F$, a winter temperature of $70 \pm 5°F$, and a humidity level around 50% can be maintained.

Turbulent Flame Burner

This burner provides a good control over initial boundary conditions, i.e., low exit turbulence intensity ($<0.25\%$) and predictable outlet velocity profile. It can be positioned precisely in x, y, and z directions (± 10 μm traversing step). It has a flexible and versatile design that is capable of accommodating a variety of experiments, such as simple one-dimensional flat-flame or complex three-dimensional recirculating flame; turbulent premixed or diffusion flames; ducted or open flames, axisymmetric or three-dimensional flow configuration; and turbulent nonreactive or reactive flow experiments.

As shown in Fig. 3, the burner is 1.5 ft high and 10 in. at its widest. It has a 4-in.-diam U-shaped inlet for annulus airflow or premixed fuel-air mixture. Four different contraction and working section pieces were designed to yield axisymmetric or three-dimensional flowfields. The blower air gives a mean exit velocity range of 5–140 m/s, and the compressed air supply

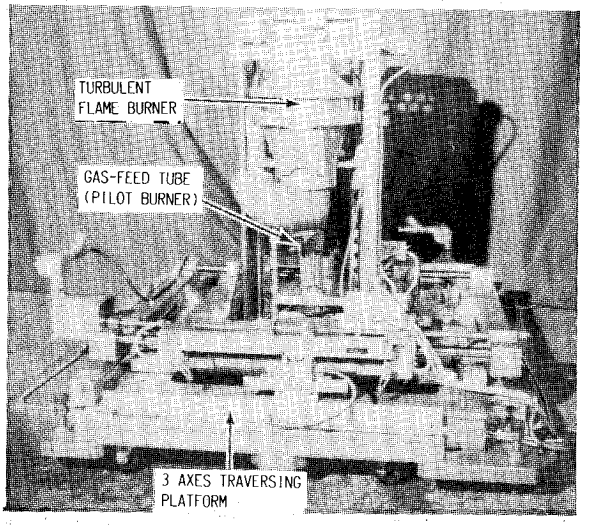

Fig. 2 Photograph showing the turbulent flame burner supported on the three-axis traversing platform.

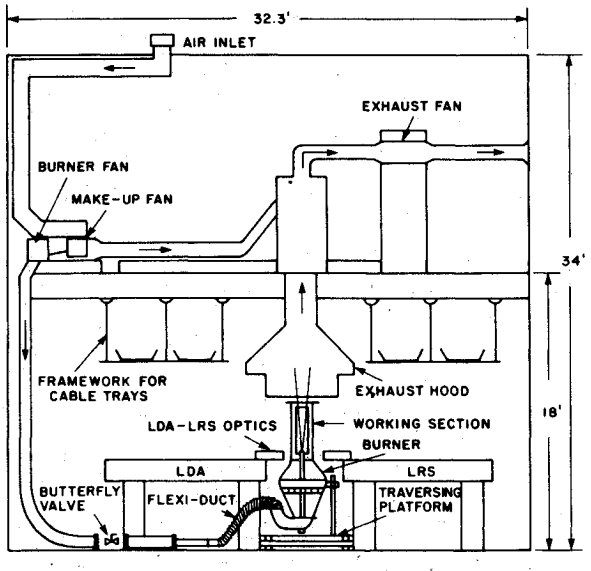

Fig. 1 Layout of the combustion laboratory.

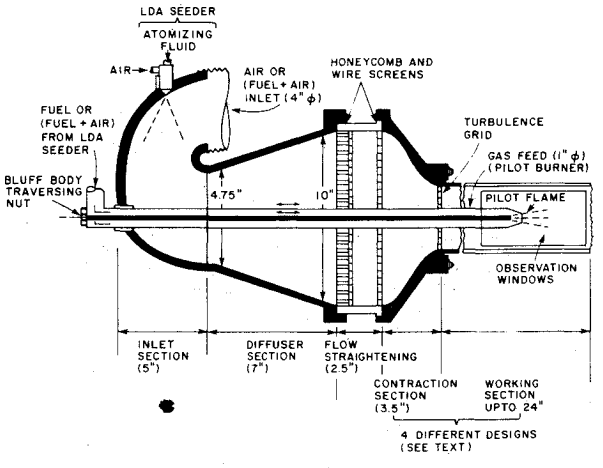

Fig. 3 Schematic diagram of the turbulent flame burner.

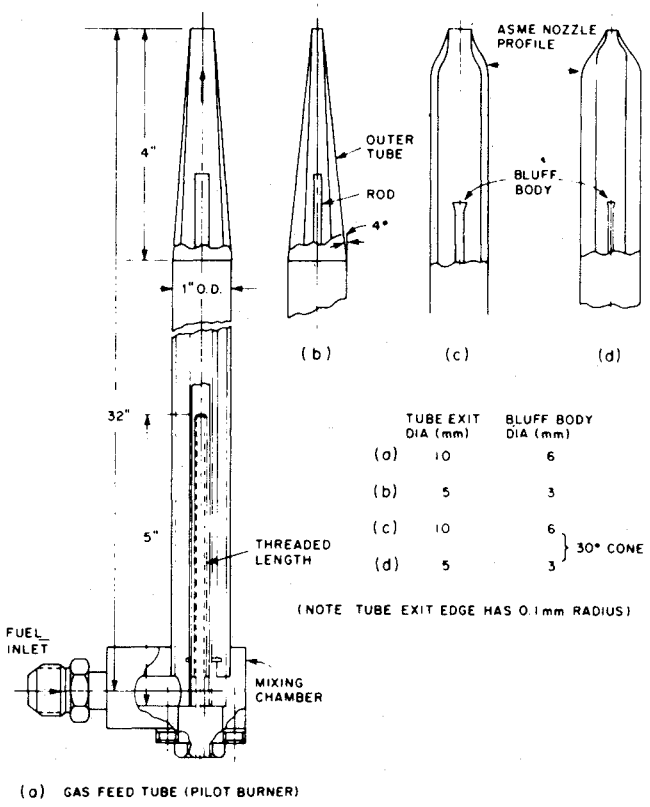

Fig. 4 Schematic diagram of the gas feed tube (pilot burner).

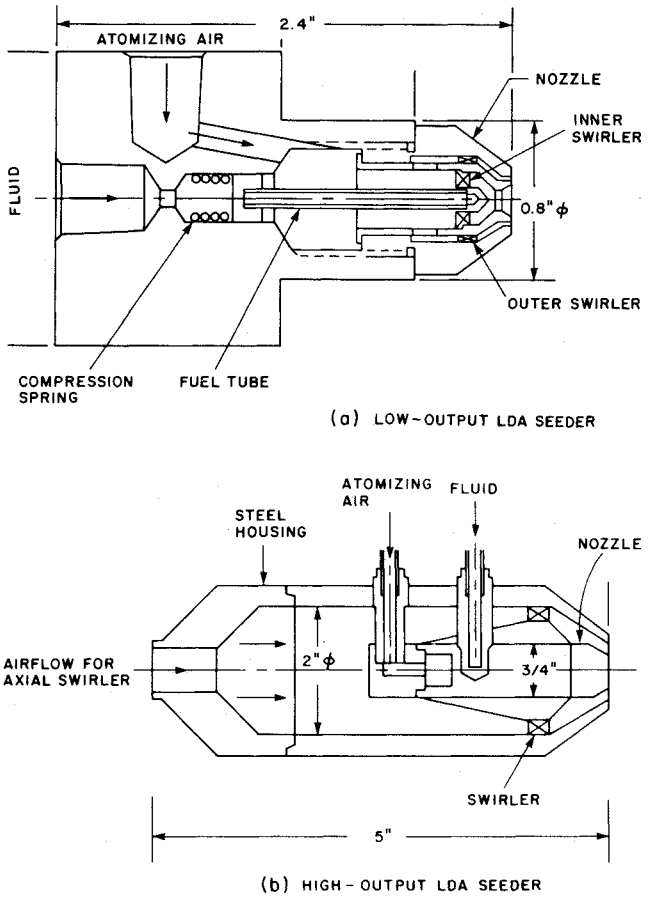

Fig. 5 Schematic diagram of the LDA seeders.

provides 1–15 m/s. To minimize the risk of a major explosion, the internal volume of the burner had to be as low as possible.

The burner has three sections: a diffuser section that reduces incoming flow velocity, a flow-straightening section that filters out large-scale and unsteady turbulence, and a contraction section that compresses the flow streamlines, suppresses axial turbulence, and produces a uniform flat mean velocity profile at its exit.

Diffuser Section

The flow through a diffuser depends upon its geometry, defined by the area ratio, wall expansion angle, cross-sectional shape, and wall contours. To keep the burner height to a minimum, a wide-angle (19 deg) diffuser was designed. The chosen angle represented the best compromise between the diffuser length and the ability of the incoming flow to fill the whole diffuser volume so that a uniform and steady flow emerged at the diffuser exit.

Flow-Straightening Section

Both screens and honeycomb grids can be used for flow straightening. Loehrke and Nagib[2] observed that maximum turbulence suppression was achieved by placing a fine gauze screen at the downstream end of the honeycomb. Therefore, a 90% porous stainless steel honeycomb with 1/16 in. hexagonal cell size and ½ in. width was specified. A 32-mesh stainless steel screen of 0.009 in. wire diam was laid on the downstream face of the honeycomb. An extra 16-mesh screen of 0.009 in. wire diam was placed 2 in. downstream of the honeycomb. Such a multiple-screen arrangement virtually eliminated large-scale turbulence. An added advantage of the multiple screens is that they are very effective in quenching any flame flashback into the settling chamber.

Contraction Section

All wind tunnels have a contraction section, because the total pressure remains constant throughout the contraction, so that both mean and fluctuating velocity variations are reduced to a smaller fraction of the average velocity at a given cross section. Contraction, also, produces a uniform reproducible exit velocity profile, i.e., a flow with well defined inlet boundary conditions.

Theoretically, it has been shown that the area contraction ratio, c ($c>1$), decreases the mean velocity variation as $(1/c)$ for u component and as $(1/\sqrt{c})$ for v and w components. The reduction in u_{rms} component of turbulence intensity is $(0.5/c)$ $[0.33\ (\ell n 4c^{-3}-1)]^{0.5}$ and in the r_{rms} or w_{rms} component it is $(3c)^{0.5}/2$. Therefore, any contraction is less efficient in suppressing longitudinal turbulence than in suppressing the mean velocity variation. Transverse fluctuations also are enhanced. To eliminate these two problems, high-quality fine honeycomb and multiple screens were located ahead of the contraction section. This significantly reduced the need for large contraction ratios. Four contraction sections ($c=2.3$, 3.0, 6.5, and 10) were designed to match corresponding working section dimensions of 15 cm square, 15 cm diam, 8.9 cm square, and 8 cm diam.

The square working section facilitates optical diagnostics, and the round cross section provides an axisymmetric flow configuration. The two larger sections are needed for producing large-scale turbulent flames of the size typically found in practical combustors and the two smaller sections are used to generate low fuel-flow-rate laboratory type flames or high velocity (up to 75 m/s) bluff-body stabilized flames.

Burner Traversing Platform

As shown in Fig. 2, the traversing platform is a three-dimensional structure machined out of thick aluminum plates.

It has a base plate to which is welded a heavy bearing block at each corner, a Y plate that slides freely on the two steel shafts held in the base plate blocks, and an X plate that moves normal to the Y plate. On the top of this third plate is bolted a 30-in. high Z superstructure. The whole burner assembly is mounted on this superstructure. Each of the three (x,y, and z) precision machined drive-screws, moving in a zero backlash type nut assembly, are coupled to an explosion proof, high-torque drive motor. The pitch of the drive screw-nut assembly, and the number of pulses of the motor were specified so that a ± 10 μm linear displacement of the burner was achieved.

Gas Feed Tube (Pilot Burner)

As shown in Fig. 4, the gas feed tube is a long stainless steel tube inserted coaxially into the burner. It has a small mixing chamber at one end in which fuel and air are premixed. At the other end, it has either a conical or an ASME type nozzle of specific inner and outer contours, Ref. (3), to produce a flat exit-velocity profile. Supported coaxially inside the tube is a steel rod threaded (and brazed to a nut) at one end with a bluff body at the other end. By mechanically rotating the nut, the bluff body can be moved 1 in. above or below the exit plane of the nozzle.

A total of four nozzle shapes were machined. These nozzles produce uniform, low turbulence and reproducible exit velocity profiles, i.e., flow with well-defined inlet boundary conditions. This gas feed tube is used in a variety of ways as follows: If a jet diffusion flame experiment is to be performed, the central rod is removed, and only fuel is inserted into the tube. For high-speed premixed turbulent flame experiments, a small pilot flame is stabilized on the bluff body, which serves to anchor a conical shaped main flame in the working section.

Burner Safety Features

This burner is designed to operate at atmospheric pressure and room temperature conditions only. Nevertheless, its casing is designed to contain all the damage in the event of an explosion. All burner sections have a gas-tight fit. Flow-straightening screens act to prevent flame flashback into the flow settling chamber. Furthermore, each gaseous fuel line (one for the annulus or outer flow and one for the gas feed tube) has triple 100-mesh fine-wire brass screen plugs installed in it to prevent flame flashback.

LDA Seeders

Small-Output Seeder

An LDA system measures the velocity of particles crossing the fringe pattern setup in the flow. Therefore, the flow has to be seeded with micron or submicron size particles capable of following the velocity fluctuations. A good LDA seeder should generate a steady flux of micron size particles and should provide control over the rate of particle generation. For combusting flow, fluidized bed seeding of refractory particles usually is employed, but this type of seeder produces large fluctuations in particle output and offers little control over the rate of particle generation.

Our LDA seeder, as illustrated in Fig. 5a, is based upon the seed particle generation technique explored by Ikioka et al.[4] We use a small Air-Swirl Prefilmer (ASP) atomizer, Model No. P/N 6830683D, Parker Hannifin Corp., Cleveland, OH. This atomizer provides excellent atomization ($< 10\mu$m) in the range 1–3 cc/min of water flow. It produces a hollow cone spray with a cone angle between 40–50 deg and uses less than 4 standard litres per minute (slpm) of air to achieve this atomization quality. A suspension of metal oxide (γ alumina or TiO_2) powder and deionized water in the proportion 4 g/l is continuously agitated by a magnetic stirrer and atomized by the ASP atomizer. The water droplets evaporate rapidly, and the seed particles are released into the flow. In our experiments, we seed both the annulus and the gas feed tube to eliminate seed biasing errors.

High-Output Seeder

A high-output seeder is required for large-scale combustion experiments. Accordingly, Fig. 5b shows an assembly sketch of this seeder. A Delavan Air Assist Nozzle No. 30609-2 is used. It has a solid spray cone angle of 40 deg at an atomizing rate in the range 5–10 cc/min. The atomizing air pressure is 3 psig and the airflow requirement is 15 slpm.

Early tests with the nozzle alone revealed its major inadequacy, namely *slow* evaporation rate of the water droplets. To rectify this deficiency, the nozzle is surrounded by a J-85 combustor dome swirler which is held in a 4 in. long 1.75 in. i.d. steel casing. This produces axially swirling motion of the outer airflow, which opens up the spray cone angle and greatly assists spray evaporation.

Fuel and Airflow Network

To design the fuel and airflow network requires knowledge of all the experiments that are planned using this network. Much thought was given to planning and visualizing numerous conceivable experiments, both nonreactive and reactive, that could be carried out using the four working sections. After doing such an exercise, ranges of fuelflow and airflow requirements were computed. These ranges are given in Table 1.

Figure 6 is a schematic diagram of the fuel and air control network. Note that a variety of fuels and inert (diluent) gases can be used in place of propane.

Design of Test Objects

To experiment with various flame geometries, different test objects were designed as follows.

Turbulence Grids

A premixed turbulent flat-flame stabilized over a grid, as shown in Fig. 7a, represents perhaps the simplest flame configuration. Here, a one-dimensional reaction zone interacts with a near-isotropic and homogeneous turbulent flow generated by a grid. This flame is amenable to rigorous mathematical analysis. Grids can be designed to produce a range of turbulence intensity and scale, i.e., a large-scale low-intensity turbulence at one extreme to a small-scale high-intensity turbulence at the other extreme. Table 2 lists the specifications of the turbulence grids.

Fuel Nozzle

The gas-feed tube shown in Fig. 7b, which runs coaxially through the burner, is used to perform axisymmetric turbulent jet diffusion flame experiments. This flame geometry is identical to the earlier work of Kent and Bilger,[5] except for the

Table 1 Fuel and airflow requirements

Experiment	Propane gasflow, kg/hr	Airflow, SCFM
Turbulent premixed flat flame	0.4–1.2[a]	5–10
	0.7–2.1[b]	8–16
	1.8–6[c]	22–40
Turbulent premixed oblique flame		
Pilot burner	0.12–1.03	1.5–8
	8.1–20[a]	110–530
Main burner	13–20[b]	175–880
	to 20[c]	490–2400
Turbulent jet diffusion flame	1.4–14[a]	110–530
	1.4–14[b]	110–900
	1.4–14[c]	250–2400

[a]Working section is 8 cm diam. [b]Working section is 8.9 cm square. [c]Working section is 15 cm square.

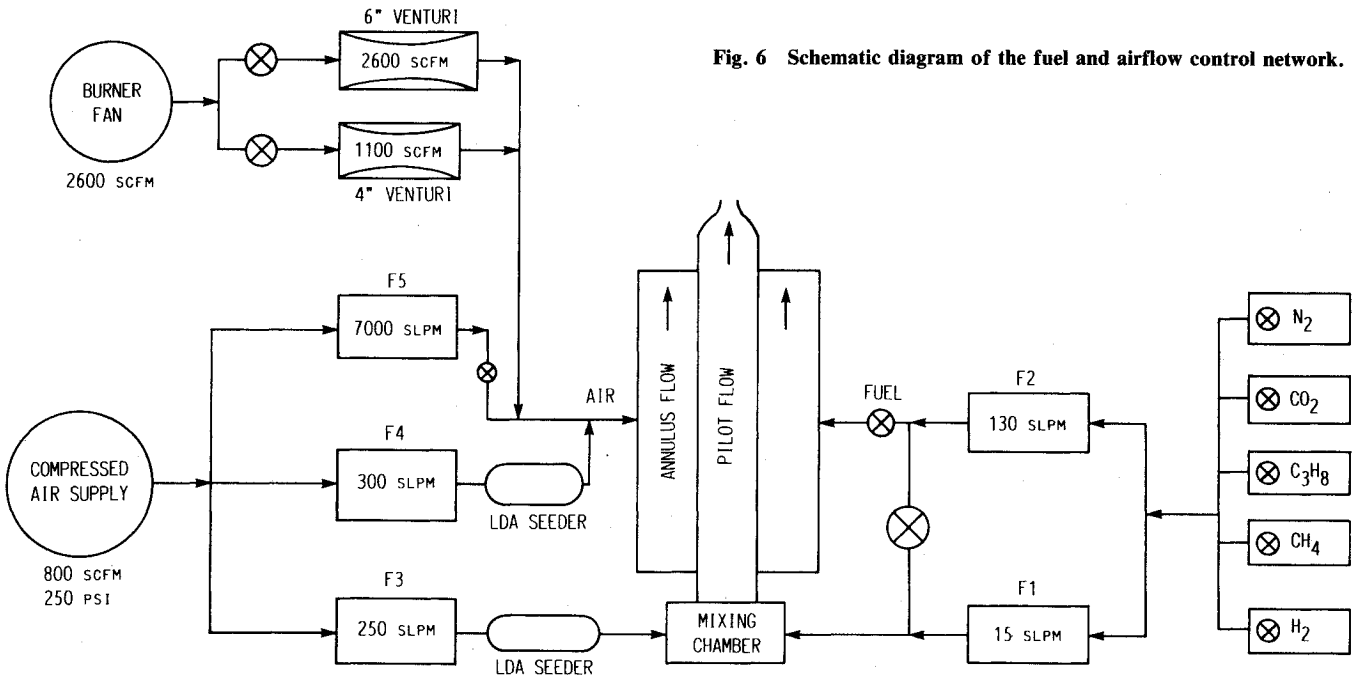

Fig. 6 Schematic diagram of the fuel and airflow control network.

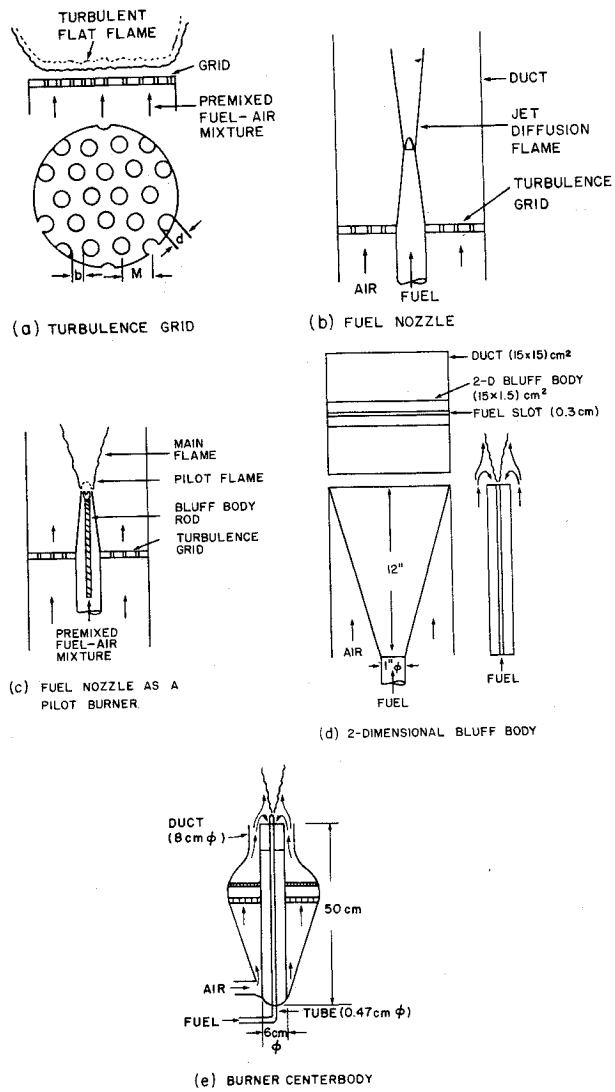

Fig. 7 Test objects fabricated to study different turbulent flame configurations.

introduction of the turbulence grid in the outer airflow to produce known levels of turbulence intensity and scale at the nozzle exit. In this way, inlet boundary conditions are changed in a controlled manner. Such experiments yield knowledge about turbulent advection, fluctuating heat release rates, and pressure gradient effects in flames.

Fuel Nozzle as a Pilot Burner

To perform experiments on high-speed turbulent flames, a pilot flame is first stabilized on the small bluff body. This anchors the main flame, as shown in Fig. 7c. Vee shaped open flames or conical shaped confined flames propagating in a grid generated turbulent flow can be produced in this manner. Study of such flames yields valuable information on the processes of turbulence suppression, generation, and dissipation in combustion.

Two-Dimensional Bluff Body

Gaseous fuel emerging from a two-dimensional slot may be entrained into the recirculation zone of a two-dimensional bluff body and ignited. As illustrated in Fig. 7d, this produces a two-dimensional diffusion flame configuration; an ideal geometry for computer code development.

Burner Centerbody

The burner centerbody, as shown in Fig. 7e, is a bullet shaped cylindrical bluff body 6 cm diam, 50 cm long with a coaxial fuel tube 1.9 cm diam running along its entire length. Gaseous fuel is injected through this tube and it mixes in the recirculation zone created by the bluff body surrounding the tube. This centerbody closely simulates the flow and the combustion environment of a gas turbine combustor dome and provides measurement access right up to its face. The centerbody is used to study the interaction between large vortices and small-scale grid turbulence, unsteady flow effects, intermittency, and recirculatory flames.

Laser Doppler Anemometer (LDA) System

LDA is a nonintrusive optical technique for measuring the velocity of the scatterer in a specific direction. If the scatterer accurately tracks the fluid motion, then the measurement is also a valid measure of the gas velocity. The principles of

Table 2 Turbulence grid specifications dimensions in in.

M	d	b	Open area	Comments
0.1	0.075	0.0287	51%	Low intensity
0.156	0.125	0.037	58%	large scale turbulence
0.187	0.140	0.054	51%	Intermediate
0.187	0.156	0.038	63%	level turbulence
0.218	0.156	0.070	46%	High intensity
0.25	0.187	0.072	51%	small scale
0.312	0.218	0.105	45%	turbulence

Table 3 LDA measurement volume dimensions

D (mm)	d_m (μm)	ℓ_m (μm)	d_f(m/s)/MHz
28.11	52	750	3.67
21.89	52	960	4.71

operation and practical aspects of measurement have been extensively explained in the literature, for example, Durst et al.[6]

The requirements of an LDA system were as follows: 1) The LDA system should be capable of measuring velocity fluctuations that span *three* orders of magnitude. This would make possible measurements in very low-velocity (~1 m/s) flat-flames at one extreme and the high-velocity (~60 m/s) pilot burner stabilized turbulent flames at the other extreme. 2) The LDA system should be capable of being integrated with the Laser Raman/Rayleigh Spectroscopy (LRS) system, i.e., to maintain their common alignment, LDA-LRS optics should be merged in such a way that fluctuations affecting one system would affect the other in the same manner. 3) At least two components of velocity (one axial) should be measured simultaneously. The LDA cannot use the 488 nm laser wavelength reserved for the LRS system. This also precludes a simple extension to a three-component LDA system.

An LDA system, satisfying these three main requirements, was built. It uses the green line of a 5 W Argon-ion laser (2 W at 514.5 nm) as a source and the two measurement channels are separated by polarization. A block diagram of the system is shown in Fig. 8a. The optical train is designed to provide three parallel optical beams with the orientation and polarization shown in Fig. 8b. The beams were brought closer using rhomb prisms (RP). The final design resulted in the two channels being formed by two sets of beams whose spacings are not equal. The system, adopted here, was the best engineering compromise.

It is preferred to collect the scattered laser radiation as close to the forward direction as possible. This maximizes the signal strength, eliminates any potential crosstalk between the channels, and preserves the polarization in the scattered radiation. In this system, the forward direction is part of the LRS multipass cell and is not accessible. Consequently, the radiation is collected at 10 deg off axis.

The spatial filter beam expander (SFBE), as shown in Fig. 8a, cleans the laser beam, expands it twofold, and focuses the beams at the crossing location so that the incident phase fronts are planar and provide linear "fringes." The beam splitters provide three beams at the vertices of a right-angle triangle. The beams were rotated to the positions shown in Fig. 8b using the 20.5 mm rhomb prisms.

The LDA measurement volume for each component has the shape of an ellipsoid of revolution with the major axis ℓ_m (along the optical axis), and the minor axis d_m. If D is the separation of the laser beams at the lens, and d_f, the fringe spacing, then our LDA measurement volume dimensions as calculated from the equations derived in Durst et. al.[6] are given in Table 3.

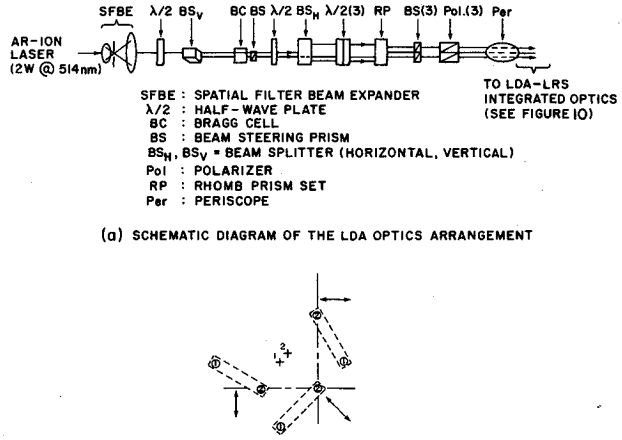

Fig. 8 Two-component LDA system.

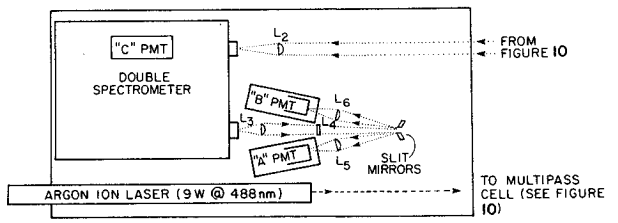

Fig. 9 Three-channel laser Raman/Rayleigh spectroscopy system.

To avoid directional ambiguity, a frequency shifter, Bragg cell operating at 40 MHz, is inserted in one leg of each LDA channel. This shifts the zero velocity signal to 40 MHz and then the actual Doppler signal lies on one side or the other of this frequency, depending upon the direction of motion of the scatterer. We also designed a phase-locked downmixer to electronically shift the signal frequency from 40 MHz to either 5 or 10 MHz. At 10 MHz, velocity resolutions of 1·1 cm/s vertically and 1·4 cm/s horizontally are obtained. These are perfectly adequate for the experiments envisioned.

Laser Raman/Rayleigh Spectroscopy (LRS) System

Figure 9 shows a photon counting three channel LRS system capable of simultaneously measuring the Rayleigh intensity and either the concentration of two gases in cold flow or the temperature and the concentration fluctuations of a single gas species, such as N_2 in a flame. It detects the pure Stokes rotational Raman lines of the probe gas, utilizing the 9 W, 488 nm line of a cw argon-ion laser and a multipass cell, which amplifies the laser power incident on the observed volume by a factor of 13 over a single pass. This combination provides signals about *three* orders of magnitude stronger than those typically observed from the N_2-Q branch using a 1 W, cw laser. The measurement volume produced by the multipass cell arrangement has a bow-tie shape and dimensions as small as 50 μm × 300μm × 1000 μm. A double spectrometer is modified to have two exit slits, and thus two identical photon counting channels become available. The third, Rayleigh channel is located in the first half of the double spectrometer. The range of wavelength spacing (~0.76 nm) of the two Raman channels, A and B in Fig. 9, is designed for measurements on the pure rotational Raman lines of the gas or gases of interest. The choice of laser wavelength of 488 nm is appropriate since there is a C_2 Swan band that overlaps the Stokes rotational Raman spectrum when the 514.5 nm line is used. The design details for the two channel optics and the multipass cell optics have been previously described by Yaney et al.[7]

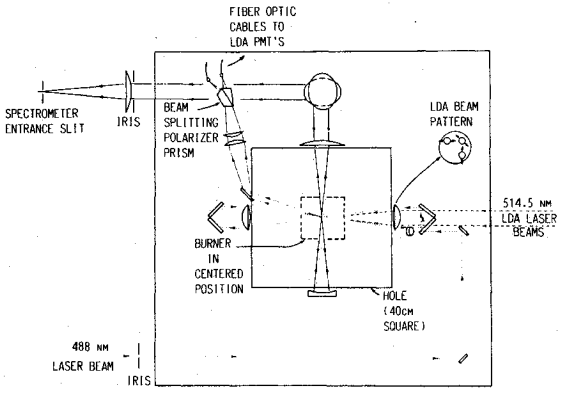

Fig. 10 Diagram illustrating the optical integration of the LDA-LRS systems.

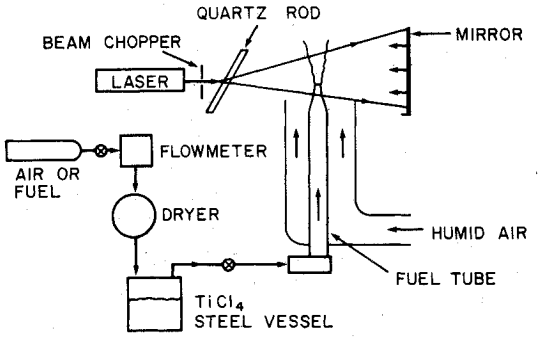

Fig. 11 Setup of the laser-sheet lighting technique for flow visualization.

Temperature measurements using two pure Stokes rotational Raman lines of nitrogen gas depends on the intensity ratio, R, of the lines. It can be shown that the temperature T is given by

$$T = K_1 / \ell n(K_2 R) \tag{4}$$

where the spacing of the lines and their rotational quantum numbers (J) determine the values of the constants K_1 and K_2.

Temperatures can also be obtained from Rayleigh measurements because the observed Rayleigh scattering intensity can be made proportional to the total number density of the gas or the absolute temperature via the ideal gas law.

If temperature is known, then Raman measurements can provide the concentration of a species in a gas. In constant temperature flows, the concentration is directly proportional to the observed Raman scattering intensity. In constant pressure flows, such as atmospheric flames, the mole fraction c of a species is given by

$$c = n_j \{ [(\lambda_j^3 \lambda_L T^2) / (\epsilon P_e \ell p)] \exp [1.4388 B_0 J(J+1)/T] \} \tag{5}$$

where n_j is the Raman count, λ_j is the wavelength of the rotational Raman line, λ_L is the wavelength of the laser light, ϵ is the calibration constant that depends on the collection geometry, the molecular species and the system detection efficiency, P_e is the excitation power in the observed volume of length ℓ and atmospheric pressure p, and $B_0 = 1.9895$ cm^{-1}, for nitrogen. These equations, the details on their use, and their range of applicability have been previously described by Yaney et al.[7]

The Raman signal detection is acomplished by two cooled photomultiplier tubes. These signals are recorded by a Modcomp Classic computer using the Raman Interface unit. This unit is a sophisticated custom designed electronic instrument, which provides all the acquisition, sequencing, and handshaking functions between the spectroscopy system and the computer.

This LRS system has many distinguishing features. It uses a simple, reliable cw laser, a high-sampling rate (up to 5 kHz in cold flows), data acquisition, has fine resolution ($\sim 30\mu$m), and good repeatability. Most important of all, this system is immune to the presence of LDA seed particles in the measurement volume, which facilitates its integration with an LDA system. Together with its software, the LRS system is capable of measuring correlation coefficients, power spectral density functions (psdfs), pdfs, and high-order moments.

LDA-LRS Integration

To measure complex quantities, such as $\overline{\rho' u'}$, $\overline{u' c'}$, and $\overline{u' T' c'}$ in turbulent flames, requires the integration of LDA and LRS systems discussed earlier. This integration has to be carried out at two levels: a) optics integration; and b) electronics/software integration.

Optics Integration

The independent optical paths of both the LDA and the LRS systems are arranged to meet at the same location so that they take measurements in the same volume. Figure 10 illustrates the optical integration of the two systems and the beam paths of the 514.5 nm (green line) LDA laser and the 488 nm (blue line) LRS laser. Important practical difficulties arise in the optical integration of these two systems. As an example, the following are four such difficulties: 1) The 488 nm light is scattered into the LRS spectrometer by the LDA seed particles. Independent tests showed that the LDA seed particles contribute only up to 3% of the Raman signal. Therefore, this problem is likely to be severe only for the Rayleigh measurements where the laser wavelength is being detected. 2) The seed particles increase the opacity to the laser light and displace the gas volume at the measurement location. Little deterioration in Raman measurements was observed. However, it would be proper to keep the seed rate as low as the LDA will allow. For Rayleigh measurements, a circuit is needed to desensitize the PMT, before the seed signal exceeds the danger level, and then quickly return the tube to full operational status. 3) Minute relative displacement or flexing among the three optic tables can occur. Although the optic tables are firmly held together by hefty steel plates, long term alignment drifts and signal degradation may result. 4) High background luminosity and unmixedness can cause deterioration of the signal levels. Our LRS system is rather immune to these effects because a narrow bandwidth (0.023–0.07 nm) is used and a large number of samples (>4096) are taken. Changes in the refractive index due to unmixedness, however, cause some deflection of the multipass-cell beams and lower its gain. Raman temperature measurements are immune to these changes since they depend only on the signal ratio; however, concentration measurements are affected.

Electronics/Software Integration

The electronic integration of the LDA-LRS signals takes place in the Raman Interface. Three modes of data acquisition are possible: 1) in the "independent" mode, the signal acquisition is controlled independently on each channel; 2) the sampling/signal acquisition clock of the Raman interface can be locked to the LDA clock. This is called the "LDA clock mode"; 3) the third acquisition mode "SYNC to LDA" provides a delayed gate or window, which is triggered by the "data ready" pulse from the LDA interface.

The schemes described above, for taking near simultaneous Raman/Rayleigh and LDA measurements, provide the choice of a software or hardware based approach. In the software based approach, a large quantity of data must be recorded;

but this record is available for unlimited trials for defining "simultaneous" measurements. In the hardware based approach, the only data that are recorded are those which are nearly simultaneous, as defined by the fixed delay and window width set on the Raman Interface.

Optical Flow Visualization System

An optical flow visualization system is used to examine the global behavior of a flow system. In this system chemical reaction of $TiCl_4$ with water vapor is used to produce micron size TiO_2 particles in the flow. These particles, which are capable of faithfully following the flow fluctuations, scatter the laser sheet-light and reveal intricate details of the flow streaklines, eddies, and vortex structures. The corrosive nature of HCl produced in the chemical reaction may have discouraged a widespread use of this method in the past. But proper handling procedure, good ventilation and exhaust systems, and using small quantities of $TiCl_4$ reduce the problem to a manageable proportion. In flames, the effect of HCl on chemical reaction/kinetic rates requires some exploration.

A schematic diagram of the experimental setup as developed by Roquemore and Chen[8] is shown in Fig. 11. A stainless steel vessel containing $TiCl_4$ is pressurized using dried and filtered compressed air. A metering valve regulates the flow of $TiCl_4$. Vapor phase $TiCl_4$ together with the moisture present in the ambient air produce the reaction $TICl_4 + 2H_2O \rightarrow TiO_2 + 4HCl$.

The optical setup, as shown in Fig. 11, consists of a cw argon-ion laser beam which strikes a quartz rod and fans out in the plane normal to the axis of the rod. In this manner, a sheet of laser light is produced. A variable speed chopper may be used to strobe this light sheet (a 20 ns Nd. Yag pulse laser has replaced this earlier arrangement) and make possible observations of repetitive or intermittent phenomenon with characteristic frequencies, such as large scale structures, and vortex shedding.

Summary and Conclusions

A versatile and sophisticated combustion laboratory has been developed at the U.S. Air Force Wright Aeronautical Laboratories, Aero Propulsion Laboratory. This facility comprises: 1) a turbulent flame burner that provides low turbulence, ($<0.25\%$), predictable outlet velocity profile, and a variety of flame configurations; 2) a two-component LDA system capable of measuring velocities with a dynamic range of over *three* orders of magnitude; 3) a three-channel LRS system capable of simultaneously measuring gas density and either the concentration of two gases in a cold flow or the temperature and concentration fluctuations of a single gas species, such as N_2, in a flame; and 4) an integration of the LDA-LRS systems.

Acknowledgments

This work was funded by the U.S. Air Force, Wright Aeronautical Laboratories, Aero Propulsion Laboratory, under Contract F33615-82-C-2255, with Dr. W.M. Roquemore serving as the Contract Monitor. A project of this magnitude could not have been completed without the direct contributions from several Air Force personnel (W.M. Roquemore, R.P. Bradley, E. Dupre, R. Parker, L. Wheeler, and J. Liffick, and D. Spohn) and other Air Force contractors (Systems Research Laboratories and Universal Energy Systems, both of Dayton, Ohio). We are deeply grateful to these individuals and organizations for their help in the different aspects of this test facility development.

References

[1]Roquemore, W.M., "Utilization of Laser Diagnostics to Evaluate Combustor Models," *AGARD—Combustion Problems in Turbine Engines,* Vol. 19, Sept. 1981, pp. 1151–1157.

[2]Loehrke, R.I. and Nagib, H.M., "Control of Free-Stream Turbulence by Means of Honeycombs," *ASME, Journal of Fluids Engineering*, Vol. 98, March 1976, pp. 342–348.

[3]Anon, "ASME Power Test Code," *Flow Measurements*, Vol. 4, ASME Publication, New York, Jan. 1959, pp. 10–15.

[4]Ikioka, L.M., Brum, R.D., and Samuelsen, G.S., "A Laser Anemometer Seeding Technique for Combustion Flows with Multiple Stream Injection," *Combustion and Flame,* Vol. 31, July 1983, pp. 78–81.

[5]Kent, J.H. and Bilger, R.W., "Turbulent Diffusion Flames," *Fourteenth Symposium (International) on Combustion,* The Combustion Institute, Pittsburgh, PA, 1972, pp. 615–624.

[6]Durst, F., Melling, A., and Whitelaw, J.H., *Principles and Practice of the Laser Doppler Anemometry,* Academic Press, New York, 1976.

[7]Yaney, P.P., Becker, R.J., Danset, P.T., Gallis, M.R., and Perez, J.I., "The Application of Rotational Raman Spectroscopy to Dynamic Measurements in Gas Flowfields," *Progress in Aeronautics and Astronautics,* Vol. 95, AIAA, New York, 1985, pp. 672–699.

[8]Roquemore, W.M. and Chen, L.D., "Visualization of Jet Flames," Paper No. 85-12, Eastern States Meeting, The Combustion Institute, Pittsburgh, PA, Nov. 1985.